



1 **Effects of ultraviolet radiation on photosynthetic performance and N₂ fixation in**
2 ***Trichodesmium erythraeum* IMS 101**

3 **Xiaoni Cai^{1,2}, David A. Hutchins², Feixue Fu² and Kunshan Gao^{1*}**

4 ¹State Key Laboratory of Marine Environmental Science, Xiamen University, Xiamen,
5 Fujian, 361102, China

6 ²Department of Biological Sciences, University of Southern California, 3616 Trousdale
7 Parkway, Los Angeles, California, 90089, USA

8 **Abstract**

9 Biological effects of ultraviolet radiation (UVR; 280–400 nm) on marine primary
10 producers are of general concern, as oceanic carbon fixers that contribute to the marine
11 biological CO₂ pump are being exposed to increasing UV irradiance due to global
12 change and ozone depletion. We investigated the effects of UV-B (280-320 nm) and
13 UV-A (320-400 nm) on the biogeochemically-critical filamentous marine N₂-fixing
14 cyanobacterium *Trichodesmium* (strain IMS101) using a solar simulator as well as
15 under natural solar radiation. Short exposure to UV-B, UV-A, or integrated total UVR
16 significantly reduced the effective quantum yield of photosystem II (PSII) and
17 photosynthetic carbon and N₂ fixation rates. Cells acclimated to low light were more
18 sensitive to UV exposure compared to high-light grown ones, which had more UV
19 absorbing compounds, most likely mycosporine-like amino acids (MAAs). After
20 acclimation under natural sunlight, the specific growth rate was lower (by up to 44%),
21 MAAs content was higher, and average trichome length was shorter (by up to 22%) in
22 the full spectrum of solar radiation with UVR, than under a photosynthetically active
23 radiation (PAR) alone treatment (400-700 nm). These results suggest that prior
24 shipboard experiments in UV-opaque containers may have substantially overestimated
25 in-situ nitrogen fixation rates by *Trichodesmium*, and that natural and anthropogenic
26 elevation of UV radiation intensity could significantly inhibit this vital source of new
27 nitrogen to the current and future oligotrophic oceans.



28 **Introduction**

29 The stratospheric ozone depletion caused by anthropogenic inputs of chlorinated
30 fluorocarbons (CFCs) and other ozone-destroying substances have resulted in an
31 increase in ultraviolet radiation reaching the Earth's surface, especially UV-B radiation
32 (280-320 nm) (McKenzie et al., 2011). Additionally, global warming is inducing
33 shoaling of the upper mixed layer and enhancing stratification, thus exposing
34 phytoplankton cells which lived in the upper mixing layer to higher depth-integrated
35 irradiance (Häder and Gao, 2015). The increased levels of UV radiation especially UV-
36 B has generated concern about its negative effects on aquatic living organisms,
37 particularly phytoplankton, which require light for energy and biomass production.

38 Cyanobacteria are the largest and most widely distributed group of photosynthetic
39 prokaryotes on the Earth, and they contribute markedly to global CO₂ and N₂ fixation
40 (Sohm et al., 2011). Fossil evidence suggests that cyanobacteria first appeared during
41 the Precambrian era (2.8 to 3.5 ×10⁹ years ago) when the atmospheric ozone shield was
42 absent (Sinha and Häder, 2008). Cyanobacteria have thus often been presumed to have
43 evolved under more elevated UV radiation conditions than any other photosynthetic
44 organisms, possibly making them better equipped to handle UV radiation.

45 Nevertheless, a number of studies have shown that UV-B not only impairs the
46 DNA, pigmentation and protein structures of cyanobacteria, but also several key
47 metabolic activities, including growth, survival, buoyancy, nitrogen metabolism, CO₂
48 uptake, and ribulose 1,5-bisphosphate carboxylase activity (Rastogi et al., 2014). To
49 deal with UV stress cyanobacteria have evolved a number of defense strategies,
50 including migration to escape from UV radiation, efficient DNA repair mechanisms,
51 programmed cell death, the production of antioxidants, and the biosynthesis of UV-
52 absorbing compounds, such as MAAs and scytonemin (Rastogi et al., 2014; Häder et
53 al., 2015).

54 The non-heterocystous cyanobacterium *Trichodesmium* plays a critical role in the



55 marine nitrogen cycle, as it is one of the major contributors to oceanic nitrogen fixation
56 (Capone et al., 1997) and furthermore is an important primary producer in the tropical
57 and sub-tropical oligotrophic oceans (Carpenter et al., 2004). This global importance of
58 *Trichodesmium* has motivated numerous studies regarding the physiological responses
59 of *Trichodesmium* to environmental factors, including visible light, phosphorus, iron,
60 temperature, and CO₂ (Kranz et al., 2010; Shi et al., 2012; Fu et al., 2014; Spungin et
61 al., 2014; Hutchins et al., 2015). However, to the best of our knowledge, nothing has
62 been documented about how UV exposure may affect *Trichodesmium*.

63 *Trichodesmium* spp. have a cosmopolitan distribution throughout much of the
64 oligotrophic tropical and subtropical oceans, where there is a high penetration of solar
65 UV-A and UV-B radiation (Carpenter et al., 2004). It also frequently forms extensive
66 surface blooms (Westberry and Siege, 2006), where it is presumably exposed to very
67 high levels of UV radiation. Moreover, in the ocean, *Trichodesmium* populations may
68 experience continuously changing irradiance intensities as a result of vertical mixing.
69 Cells photoacclimated to reduced irradiance at lower depths might be subject to solar
70 UVR damage when they are vertically delivered close to the sea surface due to mixing.
71 Therefore, this unique cyanobacterium may have developed defensive mechanisms to
72 overcome harmful effects of frequent exposures to intense UV radiation. Understanding
73 how its N₂ fixation and photosynthesis respond to UV irradiance will thus further our
74 knowledge of its ecological and biogeochemical roles in the ocean.

75 When estimating N₂ fixation using incubation experiments in the field, marine
76 scientists have typically excluded UV radiation by using incubation bottles made of
77 UV-opaque materials like polycarbonate (Capone et al., 1998; Olson et al., 2015). Thus,
78 it seems possible that most shipboard measurements of *Trichodesmium* N₂ fixation rates
79 could be overestimates of actual rates under natural UV exposure conditions in the
80 surface ocean. In this study, *Trichodesmium* was exposed to spectrally realistic
81 irradiances of UVR in laboratory experiments to examine the short-term effects of UVR
82 on photosynthesis and N₂ fixation. In addition, *Trichodesmium* was grown under natural



83 solar irradiance outdoors in order to assess UV impacts on longer timescales, and to test
84 for induction of protective mechanisms to ameliorate chronic UV exposure effects.

85

86 **Materials and methods**

87 **Study strategy** This study included two parts: (1) A short-term experiment under a
88 solar stimulator (refer to Fig.S1 for the spectrum) to examine the responses of
89 *Trichodesmium erythraeum* IMS 101 to a range of acute UV radiation exposures, and
90 (2) A long-term UV experiment under natural sunlight to examine acclimated growth
91 and physiology of *Trichodesmium* IMS 101. The first set of experiments was intended
92 to mimic intense but transitory UV exposures, as might occur sporadically during
93 vertical mixing, while the second set was intended to give insights into responses during
94 extended near-surface UV exposures, such as during a surface bloom event.

95 **Short-term UV experiment** *Trichodesmium erythraeum* IMS101 strain was isolated
96 from the North Atlantic Ocean (Prufert-Bebout et al., 1993) was maintained in
97 laboratory stock cultures in exponential growth phase in autoclaved artificial seawater
98 enrich with nitrogen free YBCII medium (Chen et al., 1996). For the short-term UV
99 experiment, the cells were grown under low light (LL) 70 $\mu\text{mol photons m}^{-2} \text{ s}^{-1}$ and
100 high light (HL) 400 $\mu\text{mol photons m}^{-2} \text{ s}^{-1}$ (12:12 light: dark) of PAR for at least 50
101 generations (about 180 days) prior to the UV experiments. These two light levels
102 represent growth sub-saturating and super-saturating levels for *Trichodesmium* (Cai et
103 al., 2015). Cultures were grown in triplicate using a dilute semi-continuous culture
104 method, with medium renewed every 4-5 days at 25°C. The cell concentration was
105 maintained at $< 5 \times 10^4 \text{ cell ml}^{-1}$.

106 To determine the short-term responses of *Trichodesmium* IMS101 to UV radiation,
107 subcultures of *Trichodesmium* IMS101 were dispensed at a final cell density of $2-4 \times$
108 $10^4 \text{ cells ml}^{-1}$ into containers that allow transmission of all or part of the UV spectrum,
109 including 35 ml quartz tubes (for measurements of carbon fixation or measurements of



110 fluorescence parameters), 100 ml quartz tubes (for pigment measurements), or 13 ml
111 gas-tight borosilicate glass vials (for N₂ fixation measurements). Three triplicated
112 radiation treatments were implemented: (1) PAB (PAR+UV-A+UV-B) treatment,
113 using tubes covered with Ultraphan film 295 (Digefra, Munich, Germany), thus
114 receiving irradiances >295 nm; (2) PA (PAR+UV-A) treatment, using tubes covered
115 with Folex 320 film (Montagefolie, Folex, Dreieich, Germany), and receiving
116 irradiances >320 nm; and (3) P treatment: tubes covered with Ultraphan film 395 (UV
117 Opak, Digefra), with samples receiving irradiances above 395 nm, representing PAR
118 (400-700 nm). Since the transmission spectrum of the borosilicate glass was similar to
119 that of Ultraphan film 295, the borosilicate glass vials for N₂ fixation measurements of
120 PAB treatment were uncovered. Transmission spectra of these tubes (quartz and
121 borosilicate) and the various cut-off foils used in this study are shown in Fig. S1.

122 The experimental tubes were placed under a solar simulator (Sol 1200W; Dr. Hönle,
123 Martinsried, Germany) at a distance of 110 cm from the lamp, and maintained in a
124 circulating water bath for temperature control (25°C) (CTP-3000, Eyela, Japan).
125 Irradiance intensities were measured with a LI-COR 2π PAR sensor (PMA2100, Solar
126 light, USA) that has channels for PAR (400-700 nm), UV-A (320-400 nm) and UV-B
127 (280-320 nm). Measured values at the 110 cm distance were 87 Wm⁻² (PAR, ca. 400
128 μmol photons m⁻² s⁻¹), 28 Wm⁻² (UV-A) and 1 Wm⁻² (UV-B), respectively. For the
129 fluorescence measurements, samples were exposed under a solar simulator for 60 min
130 and measurements of fluorescence parameters were performed during the exposure (see
131 below). Due to analytical sensitivity issues, for the carbon and N₂ incorporation
132 measurements, the exposure duration was 2 hrs, and for the measurements of UVAC
133 (UV-absorbing compounds) contents, the exposure time was 10 hrs.

134 **Long-term UV experiment** To assess the long-term effects of solar ultraviolet
135 radiation on *Trichodesmium* IMS101, an outdoor experiment was carried during the
136 winter (Jan 1st to Jan 26th, 2014) in subtropical Xiamen, China. 300-400 ml cell cultures
137 were grown in 500 ml quartz vessels exposed to 100% daytime natural solar irradiance



138 (surface ocean irradiance) (daytime PAR average of ~120W, highest PAR at noon
139 ~300W). All of the quartz vessels were placed in a shallow water bath at 25°C using a
140 temperature control system (CTP-3000, Eyela, Japan). Two triplicated radiation
141 treatments were implemented: (1) treatment P: PAR alone (400-700 nm), tubes covered
142 with Ultraphan film 395 (UV Opak, Digefra); (2) treatment PAB: PAR+UV-A+UV-B
143 (295-700 nm), unwrapped quartz tubes. Incident solar radiation was continuously
144 monitored with a broadband Eldonet filter radiometer (Eldonet XP, Real Time
145 Computer, Mährendorf, Germany) that was placed near the water bath. Daily doses of
146 solar PAR, UV-A and UV-B during the experiments are shown in Fig. S2. The
147 photoperiod during the outdoor incubation was 11:13 light:dark (light period from 7:00-
148 18:00 of local time). Cell were maintained in exponential growth phase (cell density <
149 5×10^4), with dilutions (after sunset) every 4 days. All parameters were measured after
150 acclimation under respective P or PAB radiation for a week.

151 Specific growth rate (μ , d^{-1}) of *Trichodesmium* IMS101 was determined based on
152 the change in cell concentrations over 4 days during the 8-11th and 12-15th day using
153 microscopic counts (Cai et al., 2015), the corresponding total dose from Day 8 to Day
154 11 and from Day 12 to Day 15 were 17.03 and 18.51 MJ, respectively. Chl *a* content
155 was measured at the 11th, 15th and 19th day, and Chl *a*-specific absorption spectrum was
156 measured at the 18th day. Carbon and N₂ fixation rate were measured at 11:00-13:00 on
157 the 18th day; the diel solar irradiance record on that day is given in Fig. S3. In order to
158 separate the respective effects of UV-A and UV-B on carbon and N₂ fixation, a shift
159 experiment was carried out: subcultures from either P or PAB treatments were
160 transferred into another P (PAR), PA (PAR+UV-A), PAB (PAR+UV-A+UV-B)
161 treatment, which were marked as P', PA', PAB' treatments, respectively. 35 ml quartz
162 tubes and 13 ml gas-tight borosilicate glass vials were used for carbon and N₂ fixation
163 measurements, respectively, as described below. Triplicate samples were used for each
164 radiation treatment for carbon and N₂ fixation, and the incubations were performed
165 under 100% solar irradiance for 2 hrs.



166 **Measurements and analyses**

167 **Effective photochemical quantum yield** During the exposure under the solar
168 stimulator in the short-term experiment, small aliquots of cultures (2 ml) were
169 withdrawn at time interval of 3-10 min and immediately measured (without any dark
170 adaptation) using a Pulse-Amplitude-Modulated (PAM) fluorometer (Xe-PAM, Walz,
171 Germany). The quantum yield of PSII (F_V'/F_M') was determined by measuring the
172 instant maximum fluorescence (F_M') and the steady state fluorescence (F_t) under the
173 actinic light. The maximum fluorescence (F_M') was determined using a saturating light
174 pulse ($4000 \mu\text{mol photons m}^{-2} \text{s}^{-1}$ in 0.8 s) with the actinic light level set at $400 \mu\text{mol}$
175 $\text{photons m}^{-2} \text{s}^{-1}$, similar to the PAR level during the solar simulator exposure The
176 quantum yield was calculated as: $F_V'/F_M' = (F_M' - F_t)/F_M'$ (Genty et al., 1989).

177 **Chlorophyll-specific absorption spectra and UV-absorbing compounds (UVACs)**

178 Chl *a*-specific absorption spectra were measured on the 18th day, after consecutive
179 sunny days. Cellular absorption spectra were measured using the “quantitative filter
180 technique” (Kiefer and SooHoo, 1982; Mitchell 1990). The cells were filtered onto GF/F
181 glass fiber filters and scanned from 300 to 800 nm using a 1-nm slit in a
182 spectrophotometer equipped with an integrating sphere to collect all the transmitted or
183 forward-scattered light (i.e., light diffused by the filter and the quartz diffusing plate).
184 Filters soaked in culture medium were used as blanks. Chlorophyll-specific absorption
185 cross-sections (a^*) were calculated according to Cleveland and Weidemann (1993) and
186 Anning et al., (2000). Content of Chl *a* and UV-absorbing compounds (UVACs) were
187 measured by filtering the samples onto GF/filters and subsequently extracted in 4 mL
188 of 100% methanol overnight in darkness at 4 °C. The absorption of the supernatant was
189 measured by a scanning spectrophotometer (Beckman Coulter Inc., Fullerton, CA,
190 USA). The concentration of Chl *a* was calculated according to Ritchie (2006). The main
191 absorption values for UV-absorbing compounds ranged between wavelengths of 310
192 and 360 nm, and the peak absorption value at 332 nm was used to estimate total
193 absorptivity of UVACs according to Dunlap et al., (1995). The absorptivity of UVACs



194 was finally normalized to the Chl *a* content ($\mu\text{g} (\mu\text{g Chl } a)^{-1}$).

195 *Trichodesmium* IMS101 UVACs content was compared to that of three other
196 marine phytoplankton species, including *Chlorella*.sp, *Phaeodactylum tricornutum*,
197 and *Synechococcus* WH7803, representing a green alga, a diatom and a unicellular
198 cyanobacterium, respectively. All cultures were maintained under the same conditions
199 (25°C , $150 \mu\text{mol photons m}^{-2} \text{s}^{-1}$) for several days prior to pigment extraction. The
200 absorption spectra were measured by filtering the samples on GF/filters that were
201 subsequently extracted in 4 mL of 100% methanol overnight at 4°C . The absorption
202 spectra of the supernatant were scanned from 250 to 800 nm in a spectrophotometer
203 (Beckman Coulter Inc., Fullerton, CA, USA). The Optical Density (OD) values were
204 then normalized to OD (662 nm), Chl *a* peak.

205 **Carbon fixation rates** Carbon fixation rate of both short- and long-term experiments
206 were measured using the ^{14}C method. A total of 20 ml samples were placed in 35 ml
207 quartz tubes and inoculated with $5\mu\text{Ci}$ (0.185 MBq) of labeled sodium bicarbonate (ICN
208 Radiochemicals), and were then maintained under the corresponding radiation
209 treatments for 2 hrs. After incubation, the cells were filtered onto Whatman GF/F filters
210 (Φ 25 mm) and stored at -20°C until analysis. To determine the radioactivity, the filters
211 were thawed and then exposed to HCl fumes overnight and dried at 60°C for 4 hrs
212 before being placed in scintillation cocktail (Hisafe 3, Perkin-Elmer, Shelton, CT, USA),
213 and measured with a scintillation counter (Tri-Carb 2800TR, Perkin-Elmer, Shelton,
214 CT, USA) as previously described (Cai et al., 2015).

215 **N_2 fixation rates** Rates of N_2 fixation for both short- and long-term experiments were
216 measured in parallel with the carbon fixation measurements using the acetylene
217 reduction assay (ARA) (Capone et al., 1993). Samples of 5 ml subcultures were placed
218 in 13 ml gas-tight borosilicate vials (described above), and 1ml acetylene was injected
219 into the headspace before incubating for 2 hrs under the corresponding radiation
220 treatment conditions. A $500 \mu\text{l}$ headspace sample was then analyzed in a gas



221 chromatograph equipped with a flame-ionization detector and quantified relative to an
 222 ethylene standard. The ethylene produced was calculated using the Bunsen gas
 223 solubility coefficients according to Breitbarth et al., (2004) and an ethylene production
 224 to N₂ fixation conversion factor of 4 was used to derive N₂ fixation rates, which were
 225 then normalized to cell number.

226 **Data analysis** The inhibition of ΦPSII, carbon fixation and N₂ fixation due to UVR,
 227 UV-A, or UV-B was calculated as:

$$228 \quad \text{UVR-induced inhibition} = (I_P - I_{PAB})/I_P \times 100\%$$

$$229 \quad \text{UV-A-induced inhibition} = (I_P - I_{PA})/I_P \times 100\%$$

$$230 \quad \text{UV-B-induced inhibition} = \text{UVR}_{\text{inh}} - \text{UVA}_{\text{inh}}$$

231 where I_P, I_{PA}, I_{PAB} indicate the values of carbon fixation or N₂ fixation in the P, PA
 232 and PAB treatments, respectively. Repair (r) and damage (k) rates during the 60 min
 233 exposure period in the presence of UV were calculated using the Kok model (Heraud
 234 and Beardall, 2000):

$$235 \quad P/P_{\text{initial}} = r/(r+k) + k/(r+k) \times \exp(-(r+k) \times t),$$

236 where P_{initial} and P were the yield values at the beginning and at exposure time t.
 237 Three replicates for culture conditions or each radiation conditions were used in all
 238 experiments, and the data are plotted as mean and standard deviation values. Two way
 239 ANOVA tests were used to determine the interaction between culture conditions and
 240 UVR at a significance level of p=0.05.

241

242 **Results**

243 **Short-term UV experiment** The effects of acute UVR exposure on cells grown under
 244 LL and HL conditions are shown in Fig.1. For the cells grown under LL condition, the
 245 Fv'/F_M' declined sharply within 10 min after first exposure in all radiation treatments,



246 and then leveled off. F_v'/F_M' decreased less in the samples receiving PAR alone (to 43%
247 of the initial value) than those additionally receiving UV-A (to 30% of the initial value)
248 or UV-A+UV-B (to 24% of the initial value) (Fig.1A). The F_v'/F_M' value of PA and
249 PAB treatments were significantly lower compared to the PAR treatment ($p=0.03$ and
250 $p<0.01$, respectively). F_v'/F_M' of HL grown cells declined less and more slowly
251 compared to the LL grown cells. The F_v'/F_M' of HL cells under PAR alone remained
252 more or less constant during the exposure, since the PAR level was similar to the growth
253 level of HL ($400 \mu\text{mol photons m}^{-2} \text{ s}^{-1}$). In contrast, the F_v'/F_M' decreased to 75% and
254 65% of its initial value for the PA and PAB treatment, respectively, and were
255 significantly lower than PAR treatment ($p<0.01$) (Fig.1B).

256 The damage and repair rates of the PSII reaction center estimated from the
257 exponential decay in the effective quantum yield showed higher damage and lower
258 repair rates in the LL-grown cells than in the HL-grown ones (Fig.1C,D). The PSII
259 damage rates (k , min^{-1}) of LL grown cells were 0.14, 0.16 and 0.15 min^{-1} in the P, PA
260 and PAB treatments, respectively, about 2 times faster than in the cells grown under HL
261 conditions (Fig.1C). The PSII repair rates (r , min^{-1}) of LL grown cells were 0.1, 0.06
262 and 0.05 min^{-1} in the P, PA and PAB treatments, which were 83% ($p<0.01$), 33% ($p<0.01$)
263 and 54% ($p<0.01$) lower than in HL grown cells, respectively (Fig.1D). The damage
264 rate was not significantly different among P, PA and PAB treatment within either of
265 the LL- and HL-grown treatments ($p>0.05$), but the repair rate was much higher in the
266 P treatment without UV than in PA or PAB treatments in the HL-grown cells ($p<0.01$).

267 The photosynthetic carbon fixation and N_2 fixation rates during the UV exposure
268 are shown in Fig. 2. The HL-grown cells had 17% higher photosynthetic carbon fixation
269 rates than the LL-grown ones under the PA treatment ($p<0.01$), however, the LL and
270 HL-grown cells didn't show significant differences in carbon fixation rates under the P
271 and PAB treatments ($p=0.29$, and $p=0.06$). In the presence of UV radiation, carbon
272 fixation was significantly inhibited in both LL and HL-grown cells (Fig.2A). Carbon
273 fixation inhibition induced by UV-A was about 35-45%, much larger than that induced



274 by UV-B, which caused only about a 10% inhibition of carbon fixation ($p < 0.01$). The
275 UV-A exposed carbon fixation rate was significantly higher in the LL- grown cells than
276 in HL grown cells ($p < 0.01$), while UV-B did not cause a significant difference in
277 inhibition between the HC- and LC-grown cells ($p = 0.88$) (Fig. 2B). N_2 fixation rates
278 were about twofold higher in HL-grown cells in all radiation treatments (Fig. 2C,
279 $p < 0.01$), but the UV-induced N_2 fixation inhibition showed no significant differences
280 between the LL and HL grown cells regardless of UV-A or UV-B exposures (Fig. 2D,
281 $p = 0.80, 0.62, 0.39$ for UVA-, UVB-, and UVR-induced inhibition, respectively).

282 Compared to other phytoplankton under the same growth conditions,
283 *Trichodesmium* IMS101 had much higher absorbance in the UV region (300-400 nm)
284 (Fig. 3A). In this study, the absorbance at 332 nm of HL-grown cells was about twofold
285 higher compared to LL-grown ones (Fig. 3B). However, the cellular Chl *a* content (data
286 not shown) and UVACs contents of both LL and HL grown cells did not change after
287 exposure to UV for 10 hrs (Fig. 3C).

288 **Long-term UV experiment** After being acclimated under full natural solar radiation
289 for 7 days, the specific growth rates of cells grown under the PAB treatment were
290 0.15 ± 0.01 and 0.14 ± 0.06 during the 8-11th day and 12-15th day periods, respectively.
291 These growth rates were significantly lower by 44% and 39% compared to cells grown
292 under the P treatment, respectively (Fig. 4A, $p = 0.014$ and $p = 0.03$). The mean trichome
293 lengths of PAR treatment cells on the 11th and 15th day were 758 ± 56 and 726 ± 19 μm ,
294 while addition of UVR significantly reduced the trichome length by 22% and 11%
295 ($p = 0.02$ and $p = 0.02$).

296 Analysis of the Chl *a* specific absorption spectra, $a^*(\lambda)$, demonstrated that UVR
297 had a major effect on the absorbance of UV regions and phycobilisomes (Fig. 5). The
298 optical absorption spectra revealed a series of peaks in the UV and visible wavelengths
299 corresponding to the absorption peaks of UVACs at 332 nm, Chl *a* at 437 and 664 nm,
300 phycourobilin (PUB) at 495 nm, phycoerythrobilin (PEB) at 545 nm,



301 phycoerythrocyanin (PEC) at 569 nm, and phycocyanin (PC) at 627 nm. In the UV
302 region, the $a^*(\lambda)$ value was higher in the PAB treatment cultures than in the P treatment
303 cultures (Fig. 5). The UVR treatments did not show clear effects on Chl *a* content
304 compared to acclimation to PAR alone measured on different days (Fig. S3). However,
305 the ratio of UVACs to Chl *a* was increased by 41% in the PAB compared to the P
306 treatment ($p < 0.01$).

307 The cells grown in the long-term P and PAB treatments showed different responses
308 for carbon and N_2 fixation after being transferred to short-term P', PA', and PAB'
309 radiation treatments at noon on the 18th day (Fig. 6). P and PAB acclimated cells did
310 not show significant differences in carbon fixation among all short-term P', PA', PAB'
311 treatments (Fig. 6A, $p = 0.17$, $p = 0.22$, $p = 0.51$, respectively), nor in the UV-induced
312 inhibition of carbon fixation (Fig. 6B, $p > 0.05$). However, long-term UV-A exposure
313 inhibited short-term carbon fixation by about 58% in both the P and the PAB treatments,
314 significantly higher than that induced by UV-B radiation (Fig. 6B, $p < 0.01$).

315 N_2 fixation rates of P acclimated cells were significantly higher than PAB
316 acclimated cells in all P', PA', and PAB' treatments (Fig. 6C, $p < 0.01$). The N_2 fixation
317 inhibition induced by UV-A of PAB acclimated cells was 49%, significantly higher by
318 47% than that of P acclimated cells ($p = 0.03$), while there was no significant difference
319 in UVB-induced N_2 fixation inhibition between P and PAB acclimated cells (Fig. 6D,
320 $p = 0.62$). The carbon fixation rates measured under PAR (PAR treated cells to P') and
321 PAB (PAB treated cells to PAB') conditions were 89.2 and 47.1 $\text{fmol C cell}^{-1} \text{ h}^{-1}$,
322 respectively, while N_2 fixation rates measured under those conditions were 1.9 and 0.5
323 $\text{fmol N}_2 \text{ cell}^{-1} \text{ h}^{-1}$. UVR exposure lowered estimates of carbon and N_2 fixation rates by
324 47% and 65%, respectively.

325

326 Discussion

327 Our study shows that growth, photochemistry, photosynthesis and N_2 fixation in



328 *Trichodesmium*.sp are all significantly inhibited by UVR, including both UV-A and UV-
329 B. These effects occur in both short-term, acute exposures, as well as after extended
330 exposures during acclimated growth. These results are ecologically relevant, since this
331 cyanobacterium is routinely exposed to elevated solar irradiances in its tropical habitat
332 either transiently, during vertical mixing, or over longer periods during surface blooms.
333 *Trichodesmium* provides a biogeochemically-critical source of new N to open ocean
334 food webs, so significant UV inhibition of its growth and N₂ fixation rates could have
335 major consequences for ocean biology and carbon cycling.

336 Short exposure to UVR causes a significant decline in the quantum yield of
337 photosystem II (PSII) fluorescence of *Trichodesmium*, that is consistent with damage
338 to critical PSII proteins such as D1 in a brackish water cyanobacterium *Arthrospira*
339 (*Spirulina*) *platensis* (Wu et al., 2011). UV-induced degradation of D1 proteins results
340 in inactivation of PSII, leading to reduction in photosynthetic activity (Campbell et al.,
341 1998). In addition, studies of various microbial mats have shown that Rubisco activity
342 and supply of ATP and NADPH are inhibited under UV exposure, which might also
343 lead to the reduction in photosynthetic carbon fixation (Cockell and Rothschild, 1999;
344 Sinha et al., 1996, 1997).

345 Exposure to UVR had an impact on nitrogenase activity in *Trichodesmium*, since
346 both the short- and the long-term UV exposure led to significant reduction of N₂ fixation
347 of up to 30% (short-term) or ~60% (long-term) (Fig. 2D and 6D). Studies on the
348 freshwater cyanobacterium *Anabaena*. sp. showed a 57% decline in N₂ fixation rate
349 after 30min exposure to UVR of 3.65W (Lesser, 2007). Some rice-field cyanobacteria
350 completely lost N₂ fixation activity after 25-40 min exposure to UV-B of 2.5 W (Kumar
351 et al., 2003). In our results, long-term exposure to UV led to higher inhibition of N₂
352 fixation, implying that accumulated damage to the key N₂-fixing enzyme, nitrogenase,
353 could have occurred during the growth period under solar radiation in the presence of
354 UVR.



355 Compared to N₂ fixation, UVR induced an even higher degree of inhibition of
356 carbon fixation. The carbon fixation rate decreased by 50% in the presence of UVR.
357 UV-A induced higher inhibition than UV-B, indicating that although UV-B photons
358 (295-320 nm) are in general more energetic and damaging than UV-A (320-400 nm),
359 the greater fluxes of UV-A caused more inhibition of carbon fixation, which was
360 consistent with other studies of spectral dependence of UV effects (Cullen and Neale
361 1994; Neale 2000). This finding is ecologically significant, since UV-A penetrates
362 much deeper into clear open ocean and coastal seawater than does UV-B.

363 Compared to low light-grown cells, the high light-grown ones were more resistant
364 to UVR, which was reflected in the lower PSII damage rate and faster recovery rate in
365 the presence of UVR, as well as the significantly lower levels of carbon fixation
366 inhibition caused by UV-A and/or UV-B. Such a reduced sensitivity to UVR coincided
367 well with a significant increase in UV-absorbing compounds in the HL-grown cells
368 compared to the LL-grown ones. Similar dependence of photosynthetic sensitivity to
369 UV inhibition on growth light levels has been reported in other species of
370 phytoplankton (Litchman and Neale, 2005; Sobrino and Neale, 2007). The sensitivity
371 of PSII quantum yield to UV exposure in *Synechococcus* WH7803 was also less in
372 high-light-grown versus low-light-grown cells (Garczarek et al., 2008). In addition, it
373 has been observed that phytoplankton from turbid waters or acclimated to low-light
374 conditions are more sensitive to UVR than those from clear waters (Villafane et al.,
375 2004; Litchman and Neale, 2005; Helbing et al., 2015). These observations suggest that
376 *Trichodesmium* sp. may acclimate to growth in the upper mixed layer by producing UV-
377 absorbing compounds, making them more tolerant of UVR than cells living at deeper
378 depths.

379 Although UV radiation can clearly cause damage to PSII and inhibit physiological
380 processes in *Trichodesmium* sp., this cyanobacterium has evolved protective
381 biochemical mechanisms to deal with UV radiation in their natural high-UV habitat.
382 One important class of UV-absorbing substances are mycosporine-like amino acids



383 (MAAs) and scytonemin. These compounds strongly absorb in the UV-A and/or UV-B
384 region of the spectrum, and dissipate its energy as heat without forming reactive oxygen
385 species, protecting the cells from UV and from photooxidative stress (Banaszak 2003).
386 The “mycosporine-like amino acids” (MAAs), which have strong UV-absorption
387 maxima between 310 and 362 nm (Sinha and Häler, 2008) as identified by HPLC in
388 other studies, consist of a group of small, water-soluble compounds, including asterina-
389 332 ($\lambda_{\max}=332$) and shinorine ($\lambda_{\max}=334$), which are the most abundant, as well as
390 mycosporine-glycine ($\lambda_{\max}=310$), porphyra-334 ($\lambda_{\max}=334$), and palythene
391 ($\lambda_{\max}=360$) (Shick and Dunlap 2002; Subramaniam et al., 1999). As was found
392 previously in *Trichodesmium* spp., high absorbance in the UV region is mainly due to
393 the presence of “mycosporinelike amino acids” (MAAs), with absorbance maxima
394 between 310~362 nm (Sinha and Häler, 2008).

395 Our investigation strongly suggests that *Trichodesmium* is able to synthesize
396 MAAs (λ_{\max} ~330 nm and 360 nm) in response to elevated PAR and UV radiation.
397 Synthesis of MAAs has been reported to be stimulated by high PAR and UV radiation
398 in other phytoplankton (Karsten et al., 1998; Vernet and Whitehead, 1996; Sinha et al.,
399 2001). Our high light-grown cells were more tolerant of UVR, likely at least partly due
400 to their ability to synthesize double the amount of MAAs in comparison to low light-
401 grown ones (Fig.3B). It has been showed that accumulation of MAAs may represent a
402 natural defensive system against exposure to biologically harmful UV radiation
403 (Karsten et al., 1998) and cells with high concentrations of MAAs are more resistant to
404 UVR than cells with small amounts of these compounds (Garcia-Pichel and Castenholz,
405 1993). In fact, MAAs concentrations varying between 0.9 and 8.4 $\mu\text{g mg}^{-1}$ (dry weight)
406 have been measured in cyanobacterial isolates (Garcia-Pichel and Castenholz, 1993),
407 and ratios of MAAs to Chl *a* in the range from 0.04 to 0.19 have been reported in
408 cyanobacterial mats (Quesada et al., 1999). In our study, we found that *Trichodesmium*
409 contained a much higher concentration of MAAs (the highest value in HL-grown cells
410 is 5 pg cell^{-1}) and that the ratio of these compounds to Chl *a* was 5, consisted with



411 previous reports in regard to *Trichodesmium* (Subramaniam et al., 1999), which is much
412 higher than in other phytoplankton. This adaptation could be a major reason for the
413 ability of *Trichodemium* to grow and form extensive surface blooms under strong
414 irradiation in the oligotrophic oceans.

415 In our study, no significant changes in the amount of MAAs were observed after
416 10 h of exposure to UVR under the solar simulator. In contrast, a significant increase
417 of 23% in the concentration of MAAs was observed in full solar spectrum treated cells
418 compared to PAR-treated ones grown outdoors after consecutive sunny days (on the
419 18th). It seems that the synthesis of MAAs takes a relatively long time. Other studies
420 have shown the time required for induction of MAAs in other cyanobacteria is
421 dependent on UV doses and species, and shows a circadian rhythm (Sinha et al., 2001;
422 Sinha et al., 2003).

423 Not only did long-term exposure to high solar UV radiation significantly reduce
424 *Trichodesmium*'s growth rate (by 37~44%), but it also significantly shortened its
425 average trichome length (less cell per filament) (Fig. 4). The decreased growth rates
426 correlated with decreased trichome length are consistent with our previous studies
427 under different light levels without UVR (Cai et al., 2015). It has been reported that
428 enhanced UVR is one of the environmental factors that not only inhibit the growth of
429 cyanobacteria, but also change their morphology (Rastogi et al., 2014). Study showed
430 natural solar UVR would suppress formation of heterocysts and shorten the filament
431 length of *Anabaena* sp. PCC7120 (Gao et al., 2007). Natural levels of solar UVR in the
432 Sothern China were also found to break the filaments and alter the spiral structure of
433 *Arthrospira (Spirulina) platensis*, with a compressed helix that lessens UV exposures
434 for the cells (Wu et al., 2005). Cells in the trichomes of the estuarine cyanobacterium
435 *Lyngbya aestuarii* coil and then form small bundles in response to UV-B irradiation
436 (Rath and Adhikari, 2007). However, the shortened trichomes of *Trichodesmium* in this
437 work may be a result of UV-inhibited growth rather than a responsive strategy against
438 UV.



439 Carbon fixation in the long-term experiment showed similar patterns with the
440 short-term UV experiment, demonstrating that UV-A played a larger role in inhibiting
441 carbon fixation than UV-B. Since the ratio of UV-B to UV-A is lower in natural solar
442 light (1:50) than under our artificial UVR (1:28), the inhibitory effects of UV-B were
443 smaller compared to UV-A in the cultures under sunlight. Carbon fixation and N₂
444 fixation rates measured outdoors indicated that UV-induced carbon fixation inhibition
445 recovers quickly following transfer to PAR conditions, while the UV-induced N₂
446 fixation inhibition does not (Fig.6AC). Factors that might be responsible include lower
447 turnover rate of nitrogenase than that of RuBisco; more UV-induced damage to
448 nitrogenase with lower efficiency of repair (Kumar et al., 2003); and indirect harm
449 caused by ROS (Reactive Oxygen Species) induced by UV (Singh et al., 2014).

450 The UV effects in our study were measured under conditions that minimized self-
451 shading, namely during growth as single filaments. However, in its natural habitat
452 *Trichodesmium* often grows in a colonial form, with packages of many cells held
453 together by an extracellular sheath (Capone et al., 1998). In such colonial growth forms,
454 the effective cellular pathlengths for UV radiation are likely greatly increased, thereby
455 amplifying the overall sunscreen factor for the colony. *Trichodesmium*.spp might use
456 this colony strategy to protect themselves from natural UV damage in the ocean.

457 Our investigation shows that this cyanobacterium appears to have evolved the
458 ability to produce exceptionally high levels of UV protective compounds, likely
459 mycosporine-like amino acids. However, even this protective mechanism is insufficient
460 to prevent substantial inhibition of nitrogen and carbon fixation in the high-irradiance
461 environment where this genus lives. *Trichodesmium* spp are distributed in the upper
462 layers of the euphotic zone in oligotrophic waters, and its population densities are
463 generally greatest at relatively shallow depths (20 to 40 m) in the upper water column
464 (Capone et al., 1997). It seems likely that UV inhibition therefore significantly reduces
465 the amount of critical new nitrogen supplied by *Trichodesmium* to the N-limited
466 oligotrophic gyre ecosystems, a possibility that has not been generally considered in



467 regional or global models of the marine nitrogen cycle.

468 *Trichodesmium* can form dense, extensive blooms in the surface oceans, and a
469 frequently cited estimate of global nitrogen fixation rates by *Trichodesmium* blooms is
470 $\sim 42 \text{ Tg N yr}^{-1}$ (Westberry et al., 2006). Previous biogeochemical models of global N_2
471 fixation have emphasized controls by many environmental factors, including solar PAR
472 radiation, temperature, wind speed, and nutrient concentrations (Luo et al., 2014), but
473 have largely neglected the effects of UV radiation. When estimating N_2 fixation using
474 incubation experiments in the field, however, marine scientists have typically excluded
475 UV radiation by using incubation bottles made of UV-opaque materials like
476 polycarbonate (Olson et al., 2015). Our results suggest that under solar radiation at the
477 surface ocean, including realistic levels of UVR inhibition lowers estimates of carbon
478 fixation and N_2 fixation by around 47% and 65%, respectively (Fig.6).

479 Thus, it seems likely that shipboard measurements and possibly current model
480 projections of *Trichodesmium* N_2 fixation and primary production rates that do not take
481 into account UV inhibition could be substantial overestimates. However, our study was
482 only carried out under full solar radiation, simulating sea surface conditions, so further
483 studies are needed to investigate depth-integrated UV inhibition. Moreover, the
484 response to UV radiation may be taxon-specific. For example, unicellular N_2 -fixing
485 cyanobacteria such as the genus *Crocospaera*, with smaller cell size and thus greater
486 light permeability, may be more vulnerable to UV radiation than *Trichodesmium* (Wu
487 et al., 2015). In the future, as enhanced stratification and decreasing mixed layer depth
488 expose cells to relatively higher UV levels, differential sensitivities to UV radiation
489 may result in changes in diazotroph community composition. Such UV-mediated
490 assemblage shifts could have potentially major consequences for marine productivity,
491 and for the global biogeochemical cycles of nitrogen and carbon.

492

493 **Acknowledgements**



494 This study was supported by the National Key Research Programs 2016YFA0601400
495 and National Natural Science Foundation (41430967; 41120164007) to KSG, and by
496 U.S. National Science Foundation grants OCE 1260490 and OCE 1538525 to F-X.F.
497 and D.A.H. DAH and F-X.F.'s visit to Xiamen was supported by MEL's visiting
498 scientists programs. The authors would like to thank Nana Liu and Xiangqi Yi from
499 Xiamen University for their kind assistance during the experiments.

500

501

502

503

504

505

506

507

508

509

510

511

512

513

514

515

516

517

518

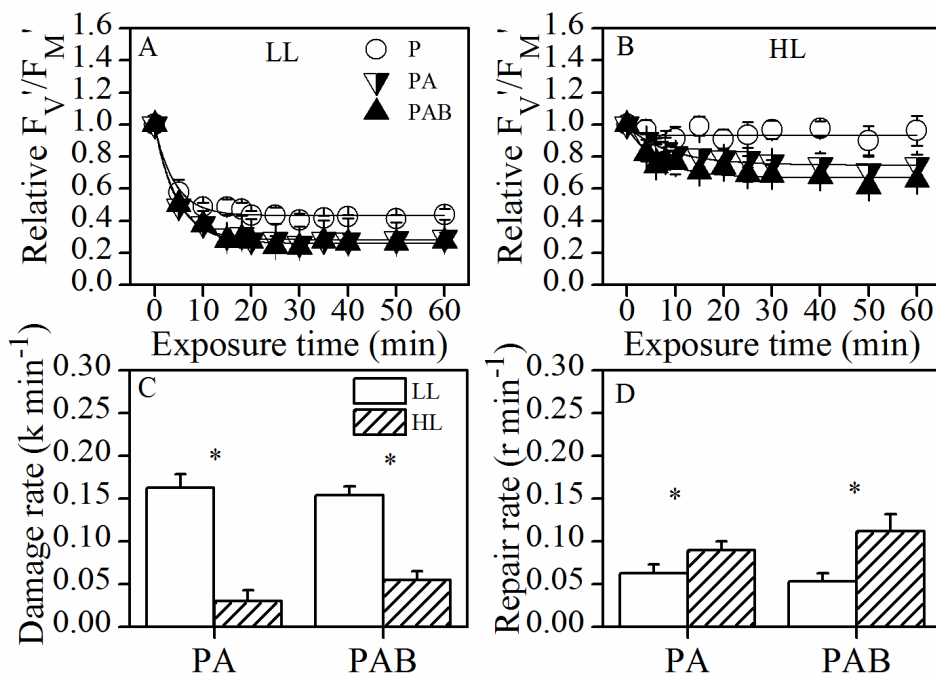
519

520

521



522 **Figures**



523
 524 Fig.1 Changes of effective quantum yield (F_v'/F_M') of *Trichodesmium* IMS101 grown
 525 under (A) LL and (B) HL conditions while exposed to PAR (P), PAR+UVA (PA) and
 526 PAR+UVA+UVB (PAB) under solar stimulator for 60 min. PSII damage (C; k , in min^{-1})
 527 and repair rates (D; r , in min^{-1}) of LL- and HL-grown cells were derived from the
 528 yield decline curve in the upper panels. Asterisks above the histogram bars indicate
 529 significant differences between LL- and HL-grown cells. Values are the mean \pm SD,
 530 triplicate incubations.

531

532

533

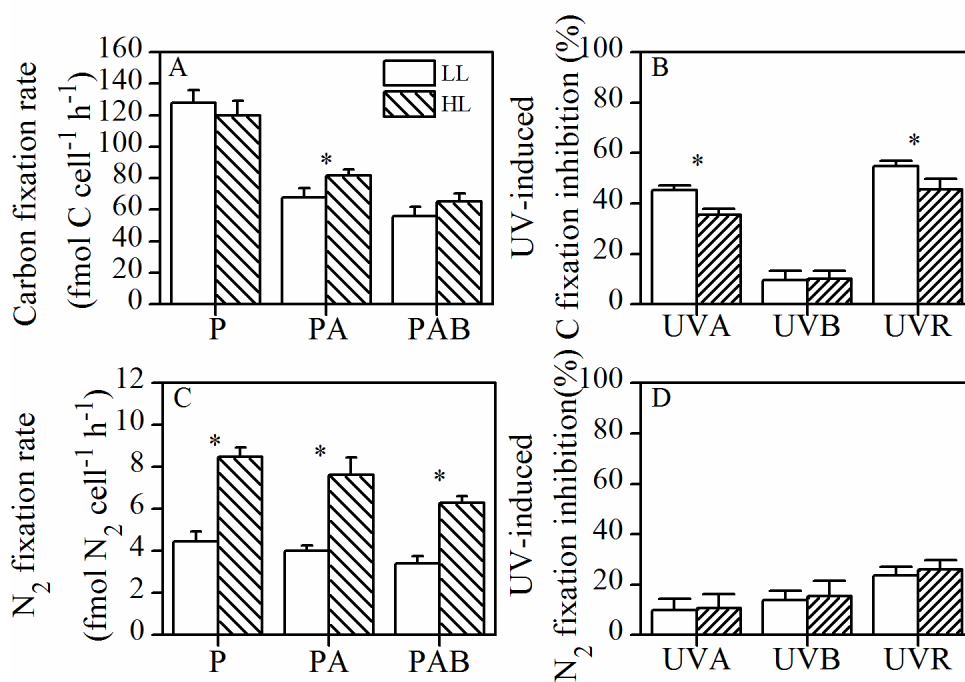
534

535

536

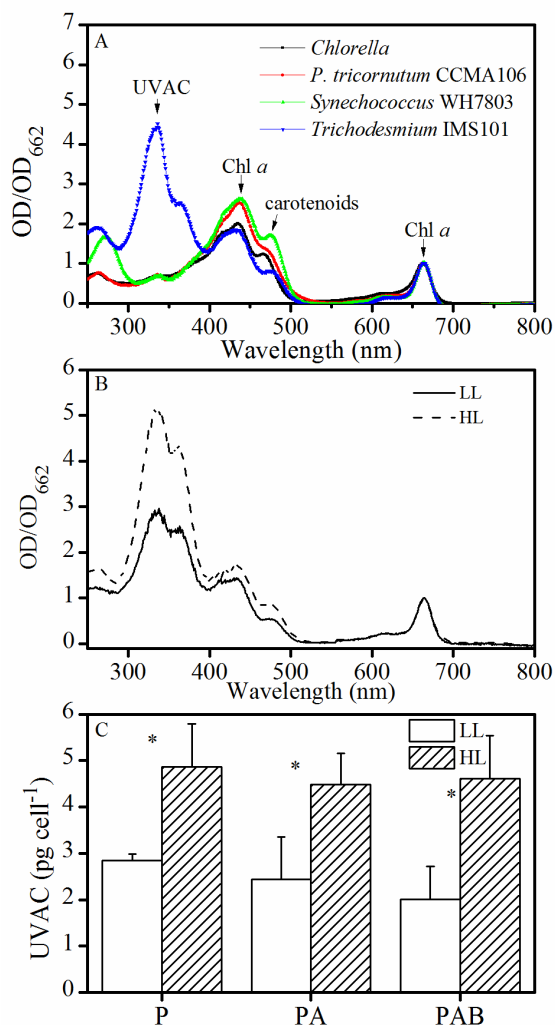


537



538

539 Fig.2 Photosynthetic carbon fixation rate (A; fmol C cell⁻¹ h⁻¹) and UV-induced C
 540 fixation inhibition (B), N₂ fixation rate (C; fmol N₂ cell⁻¹ h⁻¹) and corresponding UV-
 541 induced N₂ fixation inhibition (D) of *Trichodesmium* IMS101 grown under LL and HL
 542 conditions. Asterisks above the histogram bars indicate significant differences between
 543 LL- and HL-grown cells. Values are the mean ±SD, triplicate incubations.



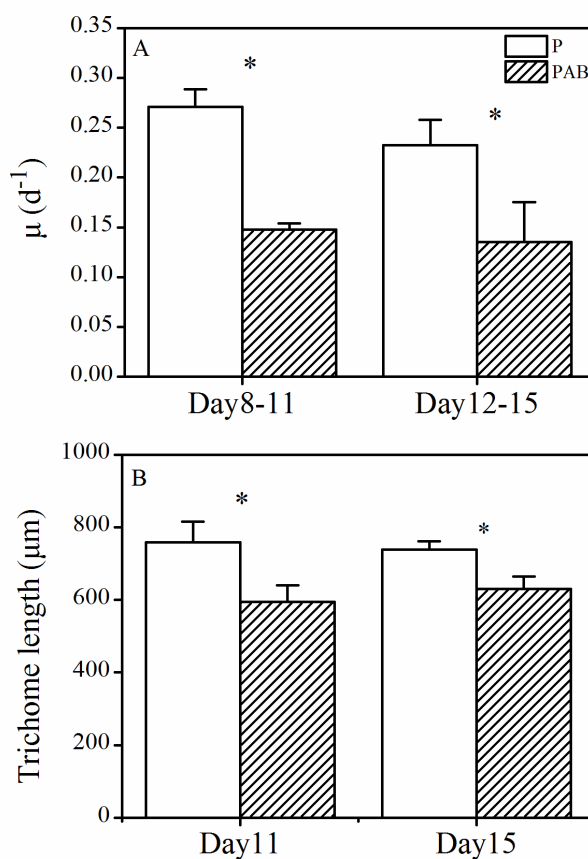
544

545 Fig.3 (A) Absorption spectrum of *Trichodesmium* IMS101 compared to other
 546 phytoplankton. Pigments were extracted by 100% methanol. OD value normalized to
 547 OD₆₆₂ (Chl *a*). (B) Absorption spectrum of the *Trichodesmium* IMS101 grown under
 548 LL and HL conditions, OD value normalized to OD₆₆₂ (Chl *a*). (C) Cellular contents of
 549 UVACs of *Trichodesmium* IMS101 grown under LL and HL conditions after exposure
 550 to PAR (P), PAR+UVA (PA), PAR+UVA+UVB (PAB) under solar simulator for 10 h.
 551 Asterisks above the histogram bars indicate significant differences between LL- and
 552 HL-grown cells. Values are the mean ±SD, triplicate incubations.



553

554



555

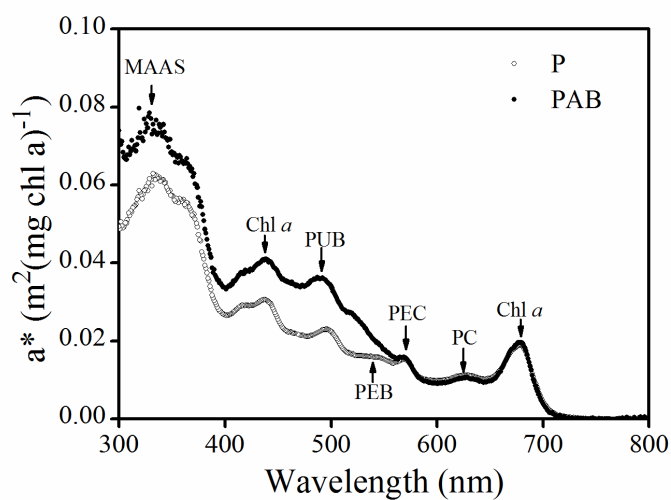
556 Fig.4 (A) Specific growth rate (measured during 8th-11th and 12th-15th day) of557 *Trichodesmium* IMS101 grown under solar PAR (P) and PAR+UVA+UVB (PAB).

558 Corresponding total solar doses from Day 8 to Day 11 and from Day 12 to Day 15 were

559 17.03 and 18.51 MJ, respectively. (B) Trichome length (measured on the 11th and 15th560 day) of *Trichodesmium* IMS101 grown under solar PAR (P) and PAR+UVA+UVB

561 (PAB). The asterisks indicate significant differences between radiation treatments.

562 Values are the mean \pm SD, triplicate cultures.



563

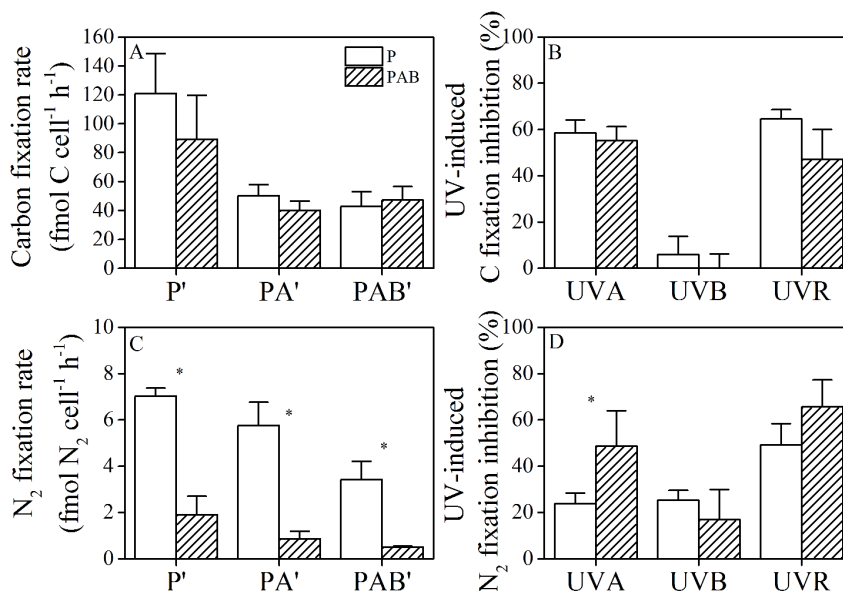
564 Fig.5 Chl *a* specific absorption spectrum (a^*) of *Trichodesmium* IMS101 grown under
 565 solar PAR (P) and PAR+UVA+UVB (PAB). The measurements were taken on the 18th
 566 day. The absorption peaks of MAAs (330 nm), PUB (495 nm), PEB (545 nm), PEC
 567 (569 nm), PC (625nm) and Chl *a* (438 and 664 nm) are indicated.

568

569

570

571



572

573 Fig. 6 Photosynthetic carbon fixation rate (A; fmol C cell⁻¹ h⁻¹) and UV-induced C
 574 fixation inhibition (B), N₂ fixation rate (C; fmol N₂ cell⁻¹ h⁻¹) and corresponding UV-
 575 induced N₂ fixation inhibition (D) of *Trichodesmium* IMS101 grown under solar PAR
 576 (P) and PAR+UVA+UVB (PAB). The measurement was taken on the 18th day at
 577 11:00~13:00. Asterisks above the histogram bars indicate significant differences
 578 between P and PAB treatments. Values are the mean ±SD, triplicate incubations.

579

580

581

582

583

584

585

586

587

588



589 **References**

- 590 1. Anning, T., MacIntyre, H. L., Sammes, S. M. P. a. P. J., Gibb, S., and Geider, R. J.:
591 Photoacclimation in the marine diatom *Skeletonema costatum*, *Limnol Oceanogr*,
592 1807-1817, 2000.
- 593 2. Bouchard, J. N., Roy, S., and Campbell, D. A.: UVB Effects on the Photosystem
594 II - D1 Protein of Phytoplankton and Natural Phytoplankton Communities,
595 *Photochem Photobiol*, 82, 936-951, 2006.
- 596 3. Breitbarth, E., Mills, M. M., Friedrichs, G., and LaRoche, J.: The Bunsen gas
597 solubility coefficient of ethylene as a function of temperature and salinity and its
598 importance for nitrogen fixation assays, *Limnol. Oceanogr. Methods*, 2, 282-288,
599 2004.
- 600 4. Cai, X., Gao, K., Fu, F., Campbell, D., Beardall, J., and Hutchins, D.: Electron
601 transport kinetics in the diazotrophic cyanobacterium *Trichodesmium* spp. grown
602 across a range of light levels, *Photosyn. Res.*, 124, 45-56, 10.1007/s11120-015-
603 0081-5, 2015.
- 604 5. Campbell, D., Eriksson, M. J., Oquist, G., Gustafsson, P., and Clarke, a. K.: The
605 cyanobacterium *Synechococcus* resists UV-B by exchanging photosystem II
606 reaction-center D1 proteins., *Proceedings of the National Academy of Sciences* 95,
607 364-369, 1998.
- 608 6. Capone, D.: Determination of nitrogenase activity in aquatic samples using the
609 acetylene reduction procedure, In P. F. Kemp, B. F. Sherr, E. B. Sherr, and J. J.
610 Cole (ed.), *Handbook of methods in aquatic microbial ecology*. Lewis Publishers,
611 Boca Raton, Fla, p. 621–631, 1993.
- 612 7. Capone, D., Zehr, J., Paerl, H., and Bergman, B.: *Trichodesmium*, a globally
613 significant marine cyanobacterium, *Science*, 276, 1221-1227, 1997.
- 614 8. Capone, D. G., Subramaniaml, A., Joseph, P., Carpenters, E. J., Johansen, M., and
615 Ronald, L.: An extensive bloom of the N₂-fixing cyanobacterium *Trichodesmium*
616 *erythraeum* in the central Arabian Sea, *Mar. Ecol. Prog. Ser.*, 172, 281-292, 1998.



- 617 9. Carpenter, E. J., Subramaniam, A., and Capone, D. G.: Biomass and primary
618 productivity of the cyanobacterium *Trichodesmium* spp. in the tropical N Atlantic
619 ocean, Deep Sea Research Part I: Oceanographic Research Papers, 51, 173-203,
620 10.1016/j.dsr.2003.10.006, 2004.
- 621 10. Chen, Y. B., Zehr, J. P., and Mellon, M.: Growth and nitrogen fixation of the
622 diazotrophic filamentous nonheterocystous cyanobacterium *Trichodesmium* sp.
623 IMS101 in defined media: evidence for a circadian rhythm, J Phycol, 32, 916-923,
624 1996.
- 625 11. Cleveland, J. S., and Weidemann, A. D.: Quantifying Absorption by Aquatic
626 Particles: A Multiple Scattering Correction for Glass-Fiber, Limnol Oceanogr, 38,
627 1321-1327, 1993.
- 628 12. Cockell, C. S., and Rothschild, L. J.: The Effects of UV Radiation A and B on
629 Diurnal Variation in Photosynthesis in Three Taxonomically and Ecologically
630 Diverse Microbial Mats, Photochem Photobiol, 69, 203-210, 10.1111/j.1751-
631 1097.1999.tb03274.x, 1999.
- 632 13. Cullen, J. J., and Neale, P. J.: Ultraviolet radiation, ozone depletion, and marine
633 photosynthesis, Photosyn. Res., 39, 303-320, 10.1007/bf00014589, 1994.
- 634 14. Dunlap, W., Rae, G., Helbling, E., Villafañe, V., and Holm-Hansen, O.: Ultraviolet-
635 absorbing compounds in natural assemblages of Antarctic phytoplankton, Antarct
636 J U S, 30, 323-326, 1995.
- 637 15. Fay, P.: Oxygen relations of nitrogen fixation in cyanobacteria, Microbiol. Rev., 56,
638 340-373, 1992.
- 639 16. Fu, F.-X., Yu, E., Garcia, N. S., Gale, J., Luo, Y., Webb, E. A., and Hutchins, D. A.:
640 Differing responses of marine N₂ fixers to warming and consequences for future
641 diazotroph community structure, Aquat. Microb. Ecol., 72, 33-46, 2014.
- 642 17. Garcia-Pichel, F., and W.Castenholz, R.: Occurrence of UV-
643 absorbing mycosporine-like compounds among cyanobacterial isolates and
644 estimation of their screening capacity, Appl. Environ. Microbiol., 163-169, 1993.



- 645 18. Genty, B., Briantais, J.-M., and Baker, N. R.: The relationship between the quantum
646 yield of photosynthetic electron transport and quenching of chlorophyll
647 fluorescence, *Biochimica et Biophysica Acta (BBA) - General Subjects*, 990, 87-
648 92, [http://dx.doi.org/10.1016/S0304-4165\(89\)80016-9](http://dx.doi.org/10.1016/S0304-4165(89)80016-9), 1989.
- 649 19. Häler, D.-P., and Gao, K.: Interactions of anthropogenic stress factors on marine
650 phytoplankton, *Frontiers in Environmental Science*, 3, 1-14, 2015.
- 651 20. Häler, D. P., Williamson, C. E., Wangberg, S. A., Rautio, M., Rose, K. C., Gao, K.,
652 Helbling, E. W., Sinha, R. P., and Worrest, R.: Effects of UV radiation on aquatic
653 ecosystems and interactions with other environmental factors, *Photochem.*
654 *Photobiol. Sci.*, 14, 108-126, [10.1039/c4pp90035a](https://doi.org/10.1039/c4pp90035a), 2015.
- 655 21. He, Y.-Y., Klisch, M., and Häler, D.-P.: Adaptation of cyanobacteria to UV-B stress
656 correlated with oxidative stress and oxidative damage., *Photochem Photobiol*, 76,
657 188-196, 2002.
- 658 22. Heraud, P., and Beardall, J.: Changes in chlorophyll fluorescence during exposure
659 of *Dunaliella tertiolecta* to UV radiation indicate a dynamic interaction between
660 damage and repair processes, *Photosyn. Res.*, 63, 123-134,
661 [10.1023/a:1006319802047](https://doi.org/10.1023/a:1006319802047), 2000.
- 662 23. Hutchins, D. A., Walworth, N. G., Webb, E. A., Saito, M. A., Moran, D., McIlvin,
663 M. R., Gale, J., and Fu, F.-X.: Irreversibly increased nitrogen fixation in
664 *Trichodesmium* experimentally adapted to elevated carbon dioxide, *Nature*
665 *Communication*, 6, 8155, [10.1038/ncomms9155](https://doi.org/10.1038/ncomms9155), 2015.
- 666 24. Karsten, U., Sawall, T., and Wiencke, C.: A survey of the distribution of UV-
667 absorbing substances in tropical macroalgae, *Phycol. Res.*, 46, 271-279,
668 [10.1046/j.1440-1835.1998.00144.x](https://doi.org/10.1046/j.1440-1835.1998.00144.x), 1998.
- 669 25. Kiefer, D. A., and SooHoo, J. B.: Spectral absorption by marine particles of coastal
670 waters of Baja California, *Limnol Oceanogr*, 27, 492-499, 1982.
- 671 26. Kranz, S. A., Levitan, O., Richter, K. U., Prasil, O., Berman-Frank, I., and Rost, B.:
672 Combined effects of CO₂ and light on the N₂-fixing cyanobacterium



- 673 *Trichodesmium* IMS101: physiological responses, *Plant Physiol.*, 154, 334-345,
674 10.1104/pp.110.159145, 2010.
- 675 27. Kumar, A., Tyagi, M. B., Jha, P. N., Srinivas, G., and Singh, A.: Inactivation of
676 cyanobacterial nitrogenase after exposure to Ultraviolet-B radiation, *Curr.*
677 *Microbiol.*, 46, 380-384, 10.1007/s00284-001-3894-8, 2003.
- 678 28. Lesser, M. P.: Effects of ultraviolet radiation on productivity and nitrogen fixation
679 in the Cyanobacterium, *Anabaena* sp. (Newton's strain), *Hydrobiologia*, 598, 1-9,
680 10.1007/s10750-007-9126-x, 2007.
- 681 29. Luo, Y.-W., Lima, I. D., Karl, D. M., and Doney, S. C.: Data-based assessment of
682 environmental controls on global marine nitrogen fixation, *BGeo*, 11, 619-708,
683 2014.
- 684 30. McKenzie, R. L., Aucamp, P. J., Bais, A. F., Bjorn, L. O., Ilyas, M., and Madronich,
685 S.: Ozone depletion and climate change: impacts on UV radiation, *Photochem.*
686 *Photobiol. Sci.*, 10, 182-198, 10.1039/C0PP90034F, 2011.
- 687 31. Mitchell, B. G.: Algorithms for determining the absorption coefficient for aquatic
688 particulates using the quantitative filter technique, Orlando'90, 16-20 April, 1990,
689 137-148,
- 690 32. Neale, P. J., and Thomas, B. C.: Inhibition by ultraviolet and photosynthetically
691 available radiation lowers model estimates of depth-integrated picophytoplankton
692 photosynthesis: global predictions for *Prochlorococcus* and *Synechococcus*, *Glob*
693 *Change Biol*, 13356, 10.1111/gcb.13356, 2016.
- 694 33. Olson, E. M., McGillicuddy, D. J., Dyrhman, S. T., Waterbury, J. B., Davis, C. S.,
695 and Solow, A. R.: The depth-distribution of nitrogen fixation by *Trichodesmium*
696 spp. colonies in the tropical-subtropical North Atlantic, *Deep Sea Research Part I:*
697 *Oceanographic Research Papers*, 104, 72-91, 10.1016/j.dsr.2015.06.012, 2015.
- 698 34. Prufert-Bebout, L., Paerl, H. W., and Lassen, C.: Growth, nitrogen fixation, and
699 spectral attenuation in cultivated *Trichodesmium* species, *Appl Environ Microb*, 59,
700 1367-1375, 1993.



- 701 35. Quesada, A., Vincent, W. F., and Lean, D. R. S.: Community and pigment structure
702 of Arctic cyanobacterial assemblages: the occurrence and distribution of UV-
703 absorbing compounds, *FEMS Microbiol. Ecol.*, 28, 315-323, 10.1111/j.1574-
704 6941.1999.tb00586.x, 1999.
- 705 36. Rastogi, R. P., Sinha, R. P., Moh, S. H., Lee, T. K., Kottuparambil, S., Kim, Y. J.,
706 Rhee, J. S., Choi, E. M., Brown, M. T., Hader, D. P., and Han, T.: Ultraviolet
707 radiation and cyanobacteria, *J. Photochem. Photobiol. B: Biol.*, 141, 154-169,
708 10.1016/j.jphotobiol.2014.09.020, 2014.
- 709 37. Rath, J., and Adhikary, S. P.: Response of the estuarine cyanobacterium *Lyngbya*
710 *aestuarii* to UV-B radiation, *J Appl Phycol*, 19, 529-536, 2007.
- 711 38. Ritchie, R. J.: Consistent sets of spectrophotometric chlorophyll equations for
712 acetone, methanol and ethanol solvents, *Photosyn. Res.*, 89, 27-41,
713 10.1007/s11120-006-9065-9, 2006.
- 714 39. Shi, D., Kranz, S. A., Kim, J. M., and Morel, F. M. M.: Ocean acidification slows
715 nitrogen fixation and growth in the dominant diazotroph *Trichodesmium* under
716 low-iron conditions, *Proceedings of the National Academy of Sciences*, 109,
717 E3094-E3100, 2012.
- 718 40. Shick, J. M., and Dunlap, W. C.: Mycosporine-like amino acids and related
719 Gadosols: biosynthesis, accumulation, and UV-protective functions in aquatic
720 organisms, *Annu Rev Physiol*, 64, 223-262,
721 10.1146/annurev.physiol.64.081501.155802, 2002.
- 722 41. Singh, S. P., Rastogi, R. P., Hader, D. P., and Sinha, R. P.: Temporal dynamics of
723 ROS biogenesis under simulated solar radiation in the cyanobacterium *Anabaena*
724 *variabilis* PCC 7937, *Protoplasma*, 251, 1223-1230, 10.1007/s00709-014-0630-
725 3, 2014.
- 726 42. Sinha, R. P., Singh, N., Kumar, A., Kumar, H. D., Häder, M., and Häder, D. P.:
727 Effects of UV irradiation on certain physiological and biochemical processes in
728 cyanobacteria, *J. Photochem. Photobiol. B: Biol.*, 32, 107-113,



- 729 [http://dx.doi.org/10.1016/1011-1344\(95\)07205-5](http://dx.doi.org/10.1016/1011-1344(95)07205-5), 1996.
- 730 43. Sinha, R. P., Singh, N., Kumar, A., Kumar, H. D., and Häder, D.-P.: Impacts of
731 ultraviolet-B irradiation on nitrogen-fixing cyanobacteria of rice paddy fields, *J*
732 *Plant Physiol*, 150, 188-193, [http://dx.doi.org/10.1016/S0176-1617\(97\)80201-5](http://dx.doi.org/10.1016/S0176-1617(97)80201-5),
733 1997.
- 734 44. Sinha, R. P., Klisch, M., Walter Helbling, E., and Häder, D.-P.: Induction of
735 mycosporine-like amino acids (MAAs) in cyanobacteria by solar ultraviolet-B
736 radiation, *J. Photochem. Photobiol. B: Biol.*, 60, 129-135,
737 [http://dx.doi.org/10.1016/S1011-1344\(01\)00137-3](http://dx.doi.org/10.1016/S1011-1344(01)00137-3), 2001.
- 738 45. Sinha, R. P., Ambasht, N. K., Sinha, J. P., Klisch, M., and Häder, D.-P.: UV-B-
739 induced synthesis of mycosporine-like amino acids in three strains of *Nodularia*
740 (cyanobacteria), *J. Photochem. Photobiol. B: Biol.*, 71, 51-58,
741 <http://dx.doi.org/10.1016/j.jphotobiol.2003.07.003>, 2003.
- 742 46. Sinha, R. P., and Häder, D.-P.: UV-protectants in cyanobacteria, *Plant Sci.*, 174,
743 278-289, [10.1016/j.plantsci.2007.12.004](http://dx.doi.org/10.1016/j.plantsci.2007.12.004), 2008.
- 744 47. Sobrino, C., and Neale, P. J.: Short-term and long-term effects of temperature on
745 photosynthesis in the diatom *Thalassiosira Pseudonana* under UVR exposures, *J*
746 *Phycol*, 43, 426-436, [10.1111/j.1529-8817.2007.00344.x](http://dx.doi.org/10.1111/j.1529-8817.2007.00344.x), 2007.
- 747 48. Sohm, J. A., Webb, E. A., and Capone, D. G.: Emerging patterns of marine nitrogen
748 fixation, *Nat Rev Microbiol*, 9, 499-508, [10.1038/nrmicro2594](http://dx.doi.org/10.1038/nrmicro2594), 2011.
- 749 49. Spungin, D., Berman-Frank, I., and Levitan, O.: *Trichodesmium's* strategies to
750 alleviate P-limitation in the future acidified oceans, *Environ. Microbiol.*, 16,
751 1935-1947, [10.1111/1462-2920.12424](http://dx.doi.org/10.1111/1462-2920.12424), 2014.
- 752 50. Subramaniam, A., Carpenter, E. J., Karentz, D., and Falkowski, P. G.: Bio-optical
753 properties of the marine diazotrophic cyanobacteria *Trichodesmium* spp. I.
754 Absorption and photosynthetic action spectra, *Limnol Oceanogr*, 44, 608-617,
755 1999.
- 756 51. Vernet, M., and Whitehead, K.: Release of ultraviolet-absorbing compounds by the



- 757 red-tide dinoflagellate *Lingulodinium polyedra*, Mar. Biol., 127, 35-44,
758 10.1007/bf00993641, 1996.
- 759 52. Villafañe, V. E., Barbieri, E. S., and Helbling, E. W.: Annual patterns of ultraviolet
760 radiation effects on temperate marine phytoplankton off Patagonia, Argentina, J
761 Plankton Res, 26, 167-174, 10.1093/plankt/fbh011, 2004.
- 762 53. Westberry, T. K., and Siegel, D. A.: Spatial and temporal distribution of
763 *Trichodesmium* blooms in the world's oceans, GBioC, 20, GB4016,
764 10.1029/2005gb002673, 2006.
- 765 54. Wu, H., Gao, K., Villafane, V. E., Watanabe, T., and Helbling, E. W.: Effects of
766 solar UV radiation on morphology and photosynthesis of filamentous
767 cyanobacterium *Arthrospira platensis*, Appl Environ Microb, 71, 5004-5013,
768 10.1128/AEM.71.9.5004-5013.2005, 2005.
- 769 55. Wu, H., Abasova, L., Cheregi, O., Deák, Z., Gao, K., and Vass, I.: D1 protein
770 turnover is involved in protection of Photosystem II against UV-B induced damage
771 in the cyanobacterium *Arthrospira (Spirulina) platensis*, J. Photochem. Photobiol.
772 B: Biol., 104, 320-325, <http://dx.doi.org/10.1016/j.jphotobiol.2011.01.004>, 2011.
- 773 56. Wu, Y., Li, Z., Du, W., and Gao, K.: Physiological response of marine centric
774 diatoms to ultraviolet radiation, with special reference to cell size, J. Photochem.
775 Photobiol. B: Biol., 153, 1-6, <http://dx.doi.org/10.1016/j.jphotobiol.2015.08.035>,
776 2015.
- 777